Methods 50 (2010) 313–322

Contents lists available at ScienceDirect

Methods

journal homepage: www.elsevier.com/locate/ymeth

Bias in the C_q value observed with hydrolysis probe based quantitative PCR can be corrected with the estimated PCR efficiency value

Jari Michael Tuomi [a], Frans Voorbraak [c], Douglas L. Jones [a,b], Jan M. Ruijter [d,*]

[a] Departments of Physiology and Pharmacology, University of Western Ontario, London, Ontario, Canada
[b] Department of Medicine, University of Western Ontario, London, Ontario, Canada
[c] Department of Medical Informatics, Academic Medical Centre, Amsterdam, The Netherlands
[d] Department of Anatomy, Embryology and Physiology, Academic Medical Centre, Meibergdreef 1105AZ, Amsterdam, The Netherlands

ARTICLE INFO

Article history:
Accepted 3 February 2010
Available online 6 February 2010

Keywords:
Hydrolysis probes
PCR efficiency
Measurement bias
Cumulative fluorescence
Quantitative real time PCR

ABSTRACT

For real-time monitoring of PCR amplification of DNA, quantitative PCR (qPCR) assays use various fluorescent reporters. DNA binding molecules and hybridization reporters (primers and probes) only fluoresce when bound to DNA and result in the non-cumulative increase in observed fluorescence. Hydrolysis reporters (TaqMan® probes and QZyme™ primers) become fluorescent during DNA elongation and the released fluorophore remains fluorescent during further cycles; this results in a cumulative increase in observed fluorescence. Although the quantification threshold is reached at a lower number of cycles when fluorescence accumulates, in qPCR analysis no distinction is made between the two types of data sets. Mathematical modeling shows that ignoring the cumulative nature of the data leaves the estimated PCR efficiency practically unaffected but will lead to at least one cycle underestimation of the quantification cycle (C_q value), corresponding to a 2-fold overestimation of target quantity. The effect on the target–reference ratio depends on the PCR efficiency of the target and reference amplicons. The leftward shift of the C_q value is dependent on the PCR efficiency and with sufficiently large C_q values, this shift is constant. This allows the C_q to be corrected and unbiased target quantities to be obtained.

1. Introduction

1.1. Background

The fluorescence-based quantitative real time PCR (qPCR) has become the gold standard technique for analysis of nucleic acids in medical diagnostics and life sciences. The proliferation of qPCR over the last decade has resulted in a diversity of reagents, protocols, analysis methods and reporting formats [1–3]. To promote consistency, increase transparency, and ensure the integrity of scientific literature, guidelines for the minimum information required for publication of qPCR experiments were formulated (MIQE) [4]. Quantitative PCR data analysis is based on the principle that the more copies of template that are present at the start, the fewer cycles of amplification it takes to make a specified amount of product [5]. The implementation of this principle involves setting of a fluorescence threshold (N_q) and determining the fractional cycle number (C_q) that is required to reach this quantification threshold [6–8]. Using the inverse of Eq. (1) (Section 4), an estimate of the target quantity (expressed in arbitrary fluorescence units) can be calculated from the observed C_q value, using the amplification efficiency and this threshold [9–11]. Almost all qPCR analyses are based on the exponential nature of PCR kinetics (Eq. (1)), and rely on the determination of the PCR efficiency per assay and C_q values per sample. However, the chemistries available for qPCR result in different kinetics of fluorescent reporter increases, which can be either non-cumulative (e.g. SYBR green) or cumulative (e.g. TaqMan® probes). Apart from the illustration of typical amplification curves obtained for amplicons detected using SYBR Green I and TaqMan chemistries [3] the cumulative nature of some monitoring chemistries is commonly ignored in qPCR data analysis.

In this paper, we outline how the cumulative nature of some reagents impacts on qPCR data analysis choices, the way the data is analyzed and the results. In short, mathematical modeling shows that ignoring the cumulative nature of the data leaves the estimated PCR efficiency practically unaffected but will lead to at least one cycle underestimation of the C_q value, corresponding to 2-fold overestimation of the target quantity. The effect on the target–reference ratio depends on the PCR efficiency of the target and reference amplicons. The leftward shift of the C_q value is dependent on the PCR efficiency and with sufficiently large C_q values, this shift is constant. This allows the C_q to be corrected and unbiased target quantities to be obtained.

* Corresponding author. Fax: +31 20 6976177.
E-mail address: j.m.ruijter@amc.uva.nl (J.M. Ruijter).

1046-2023/$ - see front matter © 2010 Elsevier Inc. All rights reserved.
doi:10.1016/j.ymeth.2010.02.003

1.2. Structure of this paper

This paper will follow the different steps of qPCR analysis from the choice of the assay to the presentation of the final results (Fig. 1). The main stream of qPCR analysis is based on determination of the PCR efficiency from standard curves (Section 2.3.1). Alternatively, PCR efficiency values can be derived from individual amplification curves (Section 2.3.2). The calculation steps in the flow chart explicitly separate the calculation of the target quantity of the gene of interest and reference genes from the calculation of the gene expression ratio. Many qPCR algorithms immediately calculate the expression ratio, thereby simplifying the equations by leaving out the quantification threshold and the PCR efficiency values. These equations inadvertently suggest that differences in PCR efficiency values do not play a role and can be ignored. It should be kept in mind that such simplification of the equations can only be done when the PCR efficiencies are equal [11]. Even small differences in efficiency can have a large effect on gene expression ratios [7].

Each section of the text will focus on a step, review the aspects relevant in the comparison of cumulative and non-cumulative chemistries and detail how the chosen detection chemistry will impact on the procedure and affect the result. Most steps will be illustrated with experimental or simulated data and graphs showing the biasing effect of the use of accumulated fluorescence data. Recommendations or correction methods will be presented where possible. These sections will refer to Section 3 describing the qPCR experiment of which the data are shown to illustrate certain steps and to Section 4 describing the basic and derived equations used in qPCR data analysis and in the correction of the biasing effects of cumulative fluorescence data.

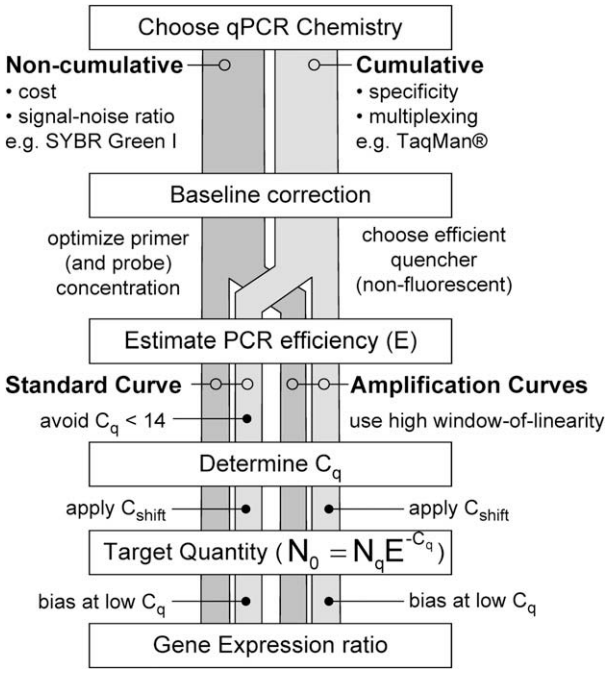

Fig. 1. *Flow chart:* graphical illustration of the six decision and calculation steps in a quantitative PCR experiment that are described in this paper. The choice for a PCR monitoring chemistry results in the use of a non-cumulative or a cumulative reporter-fluorescence increase during PCR which has implications for the baseline subtraction. A second choice has to be made between PCR efficiency estimation with a standard curve or estimation from the amplification curves. Both methods can be applied to non-cumulative as well as cumulative fluorescence data. After determination of the C_q values and calculation of the target quantities, all data streams come together in the calculation of the gene expression ratio which is the final result of a qPCR experiment.

2. Quantitative PCR analysis steps

2.1. Choice of detection chemistry

An impressive variety of monitoring chemistries are available for qPCR. The available non-cumulative fluorescent detection technologies depend on two principle mechanisms: (1) where a dye fluoresces upon binding with double stranded DNA (e.g. SYBR green), and (2) where fluorescence increases upon hybridization of the reporter to a specific oligonucleotide sequence. Examples of the latter include hairpin probe hybridization (LUX, Light Upon eXtension, Invitrogen), hairpin loop hybridization (Molecular beacons [12], Sigma Aldrich/IDT), and dual probe hybridization (Light Cycler, Roche) [2]. As the structure of these fluorescent reporters remains intact during the PCR reaction, the resulting increase in signal intensity is directly proportional to the amount of amplification product.

Cumulative reporter technologies depend on a hydrolysis step that irreversibly separates a fluorescent reporter from a quencher molecule. The close proximity of reporter and quencher, maintained until hydrolysis, results in suppression of the reporter molecule fluorescence (see Section 2.2). Examples of hydrolysis based chemistries include TaqMan® probes (Applied Biosystems), and the QZyme™ assay (Clontech laboratories, Inc.). As of December 2009, a PubMed search for TaqMan® probe-based assays yielded 4180 hits, while application of the QZyme™ assay has not yet gained popularity yielding only two PubMed hits. During the annealing/extension phase of PCR, the TaqMan® probe hybridizes to the template and the double stranded DNA-specific 5′–3′ exonuclease activity of thermostable Taq or Tth polymerase degrades the probe and releases the reporter. The increased specificity due to the requirement for matching three independent nucleotide sequences (forward and reverse primers and probe), and the ability to multiplex reactions using different fluorophores in TaqMan® assays underlies the popularity of this system [2,13].

The cumulative fluorescence of hydrolysis reporters leads to observed fluorescence values that are higher than the kinetic equation of PCR predicts. Assuming the same fluorescence characteristics for a cumulative and a non-cumulative signal, Fig. 2A shows a simulation of the amplification curves of the same target, monitored with non-cumulative fluorescent dye binding (Eq. (1)) and with a cumulative fluorescent probe (Eq. (2)). The PCR efficiency and target quantity N_0 was the same for both lines. At high cycle numbers, the lines become practically parallel on a logarithmic scale. The almost constant distance between the lines approximates a limit, written as ΔN. The mathematical derivation (see Appendix A) of this limit leads to Eq. (3), showing that ΔN is only dependent on the PCR efficiency. The distance between the non-cumulative and cumulative fluorescence curves for different PCR efficiency values is plotted in Fig. 2B. The horizontal lines represent the respective ΔN values calculated with Eq. (3). The graph shows that for a PCR efficiency of 1.4, parallelism can be considered to be reached after 20 cycles whereas at maximum PCR efficiency as little as 11 cycles are sufficient to reach parallelism. This means that for most quantitative PCR applications, on a semi-logarithmic plot the curves can be considered to be parallel at the level of the quantification threshold.

2.2. Baseline correction

Baseline fluorescence is defined as the level of fluorescence measured before any specific amplification can be detected. The word ‘baseline’ is used to avoid confusion with the ‘background’ which in PCR systems is often used to address the fluorescence of the internal reference dye (e.g. ROX or Fluorescein) or the signal

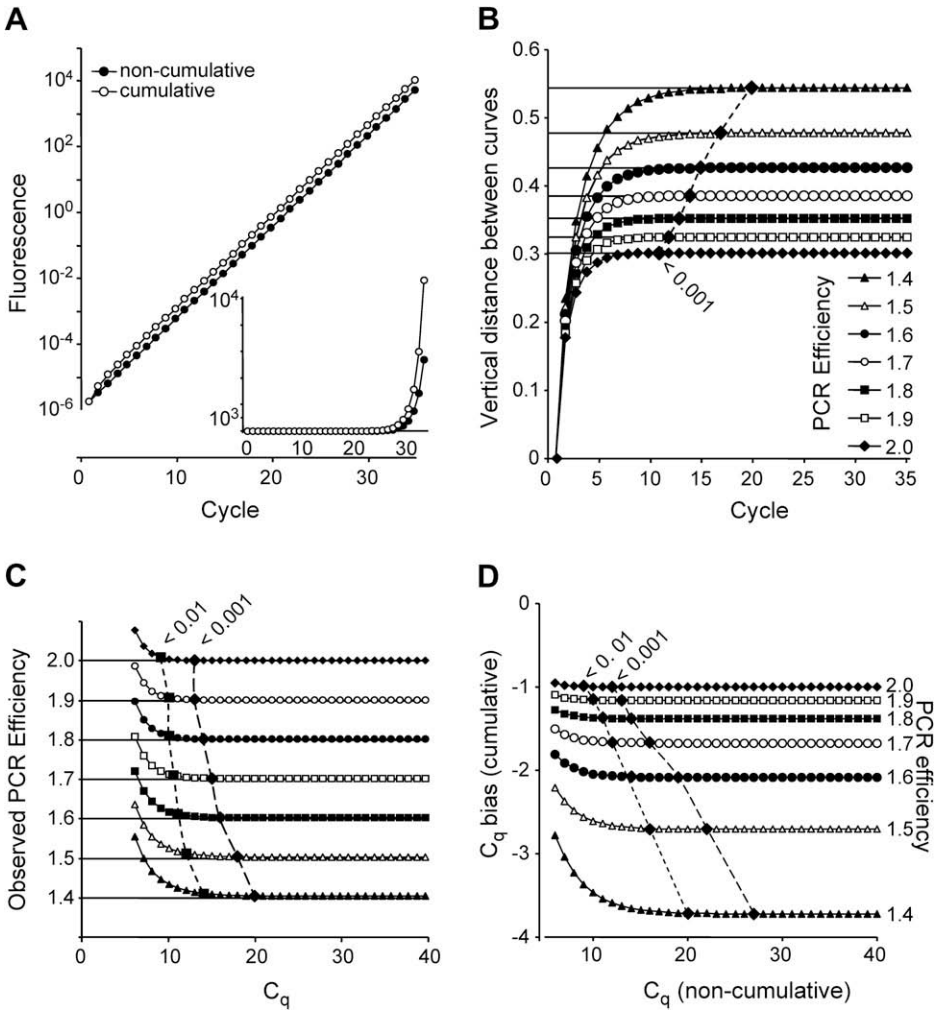

Fig. 2. PCR efficiencies derived from non-cumulative and cumulative fluorescence curves. (A) Graphical representation of Eqs. (1) and (2) (Section 4) showing that on a logarithmic fluorescence axis, the curves resulting from a non-cumulative and a cumulative monitoring chemistry become virtually parallel. The inset shows the same data on a normal Y-axis. Parameters: N_0: 0.000001, PCR Efficiency: 1.9 for both curves. (B) Demonstration that the vertical distance between the logarithmic curves closely approaches ΔN after a number of cycles that depends on the PCR efficiency. For each efficiency value, the black diamond indicates when the actual distance is less than 0.001 from ΔN. (C) PCR efficiencies derived from a subset of 4 cumulative fluorescence data points according to the window-of-linearity approach [34]. The PCR efficiencies are plotted against a C_q value obtained by placing a quantification threshold one cycle below the upper limit of the data window. In windows that include early cycles the observed PCR efficiencies show a positive bias. The large black squares and diamonds indicate the C_q cycles above which this bias is less than 1% and 0.1%, respectively. Parameters: N_0: 0.000001, PCR Efficiency: 1.4–2.0. (D) Bias in observed quantification cycle (C_q) for cumulative fluorescence data. C_q values in the simulated cumulative dataset were determined for quantification thresholds that lead to integer C_q values in a simulated non-cumulative data set. The large diamonds indicate the cycles at which the biases differ less than 0.001 from the C_{shift} predicted by Eq. (4) for each of the included PCR efficiency values. Parameters: N_0: 0.000001, PCR Efficiency: 1.4–2.0.

observed outside the reaction wells. Similarly, the fluorescence baseline should not be confused with background defined as the amplification resulting from a 'non-template', 'minus RT' or 'water' control samples [14].

Fluorescence baseline has been described as constant, linearly dependent on cycle number [15–17] or as a non-linear saturation curve [18,19]. The definition of a constant baseline ranges from the minimum observed fluorescence [20], the mean of the five lowest observations [21], the mean of a fixed set of cycles [22,23] and the mean value of a dynamically determined set of ground phase cycles [15]. Most qPCR systems currently use a linear baseline trend.

It was described previously that a 2% underestimation of the baseline leads to a 2% underestimation of the PCR efficiency determined from the amplification curves whereas a similar overestimation of the baseline leads to such an overestimation of the PCR efficiency. Because of the exponential nature of PCR, such errors in the PCR efficiency can lead to a 10-fold error in reported gene expression ratios. To avoid these baseline estimation errors a new estimation algorithm was described [24]. This baseline estimation algorithm is based on the kinetic model of PCR amplification (Eq. (1)) and assumes that the observed fluorescence at each data point up till the start of the plateau phase is the sum of baseline fluorescence and an exponential increasing amplicon concentration dependent fluorescence. The constant PCR efficiency in the exponential phase means that, in a semi-logarithmic plot, the data points in the exponential phase of the PCR reaction are on a straight line. The correct baseline value isolates the exponentially increasing part of the observed fluorescence values and results in the longest straight line of data points downwards from the plateau phase [24].

Experimental data from mouse atrium samples were analyzed using both SYBR green as well as TaqMan® assays (see Section 3). The raw fluorescence data show that the baseline-to-plateau distance in SYBR green fluorescence data is larger than in TaqMan® data (Fig. 3A). A similar difference in baseline-to-plateau distance between the two monitoring chemistries has been illustrated in other papers [3]. After baseline correction [24], both data sets show

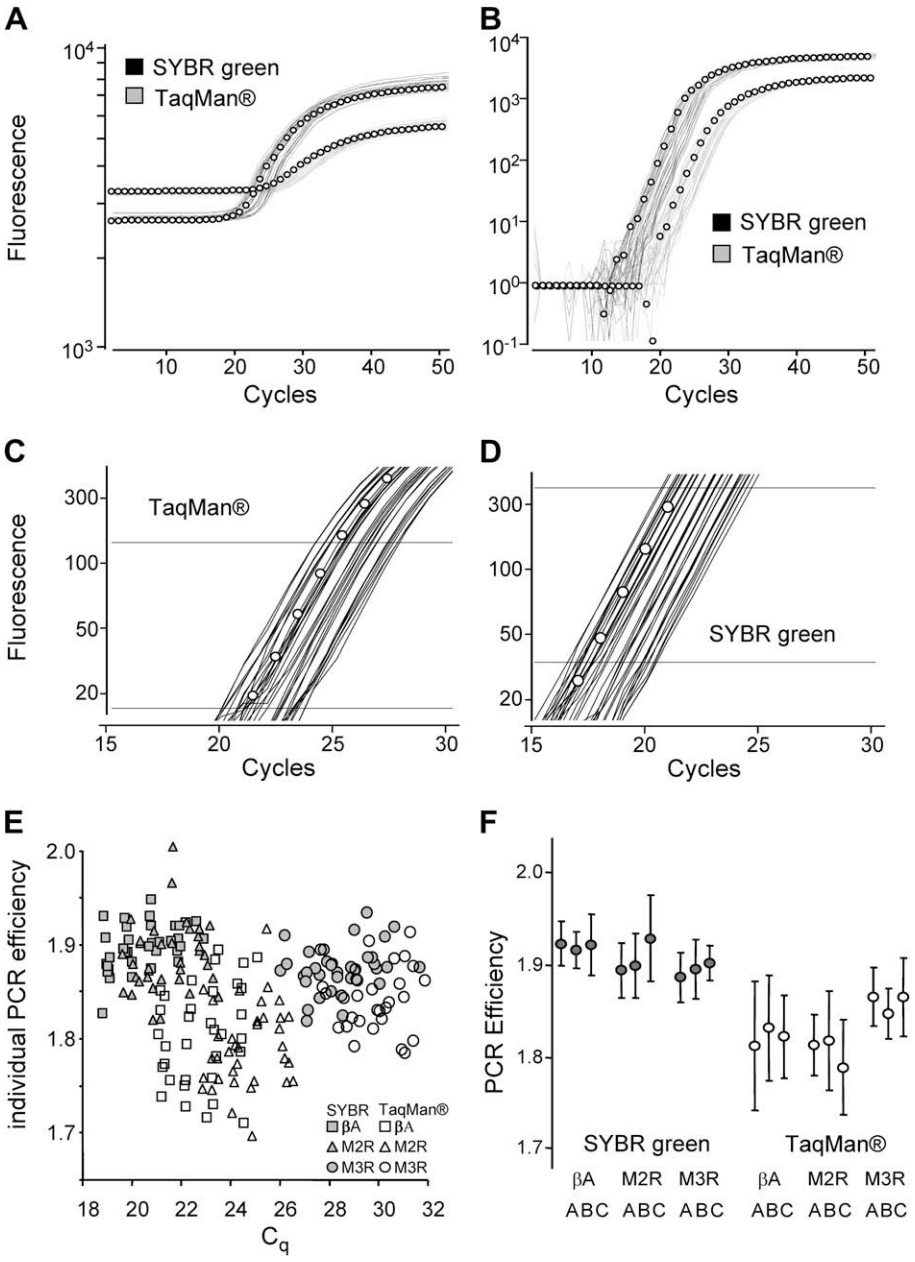

Fig. 3. qPCR analysis with SYBR green and TaqMan® hydrolysis probe assays. Amplification curves resulting from an experiment in which three amplicons (β-actin, M2 muscarinic receptor and M3 muscarinic receptor) were amplified with a non-cumulative SYBR green assay and a cumulative TaqMan® hydrolysis probe assay. Details on biological samples, experimental design and reaction conditions are given in Section 3. (A) Raw fluorescence data resulting from PCR amplification of the M2 muscarinic receptor. The data are plotted on a logarithmic fluorescence axis and show that SYBR green fluorescence results in a larger baseline-to-plateau distance than TaqMan®. (B) Data from panel A were baseline corrected [24] and plotted on a logarithmic fluorescence axis. (C) Detail of the part of the TaqMan® amplification curves that is used for determination of the PCR efficiency per sample. The horizontal lines indicate the window-of-linearity [24]. Note that, although the window is at the top of the exponential phase, the amplification curves at the bottom of the window are diverging. (D) As C but for SYBR green amplification curves. Within the window virtually all amplification curves are parallel. (E) PCR efficiencies and C_q values determined for both assays and the three amplicons. The plot of PCR efficiency against C_q value shows no correlation between these two parameters. (F) Mean PCR efficiency (with 1 times standard deviation; $N = 12$ per amplicon per sample) observed for a SYBR green and a TaqMan® hydrolysis probe assay. The graph shows that PCR efficiencies per sample overlap per amplicon, indicating the PCR efficiency is not sample dependent. Although the PCR distributions overlap for all amplicons in the SYBR Green assay and between β-actin and the M2 muscarinic receptor for the TaqMan® assay, those of the M3 muscarinic receptor in the TaqMan® assay are significantly higher. Therefore, PCR efficiencies should be considered to differ between amplicons and between monitoring chemistries.

an exponential phase ranging over approximately 10 cycles (Fig. 3B).

An important factor influencing the baseline estimation is the baseline-to-plateau distance (ΔR_n) in the raw, i.e. not baseline corrected, data. This distance is determined by intrinsic properties of the fluorescent reporter and on the primer and probe concentrations [24]. For non-cumulative fluorescence data, a large part of the baseline fluorescence results from the fluorescence of the unbound fluorochrome or fluorescent probe. For example, the unbound molecule of the DNA binding dye SYBR green is already fluorescent but at only 1/1000 of the fluorescence of the bound molecule [25]. High ΔR_n values are typical of SYBR green chemistry [3]. ΔR_n values recorded with hydrolysis probes, however, are reported to be significantly lower due to the use of FRET based chemistries that display inefficient quenching. For these chemistries it is important to choose a reporter/quencher pair that gives the largest

baseline-to-plateau difference. This will facilitate the estimation of the correct baseline value and thus reduce the variation in observed PCR efficiency values (Fig. 3F) [24].

Criteria for selection of reporter/quencher pairs that display efficient quenching have been described. Briefly, three mechanisms of quenching reporter fluorescence include; (1) fluorescent resonance energy transfer (FRET); (2) static or contact quenching, and (3) quenching by the nucleotide proximal to the fluorophore (Guanine for FAM, Adenine for Alexa-488 dyes) [26]. In order to achieve efficient FRET, the reporter and quencher must be close to one another, and the absorption spectrum of the quencher must overlap the emission spectrum of the reporter fluorophore [27,28]. Reporter and quencher molecules can bind to form a ground-state complex [29]. Such coupling of the reporter and quencher's excited-state energy levels results in different electronic properties of the ground-state complex that inhibits fluorescence [29]. The efficiency of contact quenching was revealed to always be greater than the efficiency of quenching by FRET [27,29].

Conventional TaqMan® probes use the reporter fluorophore, fluorescein (FAM), and a quencher, tetramethylrhodamine (TAMRA), which is also fluorescent. FAM/TAMRA based probes display relatively efficient quenching, over 90% [29]; however, the remaining unquenched FAM and fluorescent TAMRA contribute significantly to baseline fluorescence and decrease ΔR_n. Non-fluorescent 'dark' quenchers absorb light and emit only heat [30]. These dark quenchers, trademarked black hole quenchers (BHQ®; Biosearch Technologies) can greatly increase signal to noise ratios in qPCR.

2.3. PCR efficiency estimation

For the transformation of qPCR data into (relative) target gene quantity, almost all qPCR data analyses are based on estimating PCR efficiencies, setting an N_q threshold and determining the C_q value per sample [17,31]. The calculation of the target gene quantity N_0, uses the inverse of Eq. (1) ($N_0 = N_q/E^{C_q}$) and a PCR efficiency E, for which several estimation methods have been proposed in the literature.

Some qPCR data analysis algorithms, such as the comparative C_q method [32], use equations that do not account for specific PCR efficiency values. However, the derivation of these equations requires the efficiency values for all amplicons to be equal or even equal to 2. The MIQE guidelines do not mention an acceptable range of PCR efficiency values [4]. For the comparative C_q method a validation method to test the equality of target and reference efficiency was described [6]; at a PCR efficiency of 1.8, an observed efficiency up to 1.83 meets this criterion. Recently a range of 1.93–2.05 for the standard curve-derived efficiency was described to reflect an optimized assay [3]. Note, however, that at a C_q of 30 cycles, treating an actual PCR efficiency of 1.9 as if maximal amplification was reached leads to an approximately five-times overestimation of the target quantity [7]. When a small over-or underestimation of the PCR efficiency occurs independently in the target and reference genes, a 10-fold error in the gene expression ratio can easily result [24]. It may be for this reason that the comparative C_q method is described as the most popular but not necessarily the most appropriate method [4].

Several reports showed that the assumption that the amplification efficiencies of the amplicon of interest and the reference gene were similar enough to ignore the differences, resulted in over- as well as under estimations of the biological effects [11,24,32–35]. To avoid this bias analysis should be based on a PCR efficiency value per amplicon [9–11,36,37].

2.3.1. PCR efficiency derived from a standard curve

The PCR efficiency per amplicon is most often derived from a dilution series, also known as standard curve [38] which is a plot of C_q values versus the known log-concentration of a series of known concentrations or a serial dilution of a standard sample [3,6,32,36,39,40]. The simplicity and general use of the standard curve has led to its implementation in qPCR software which has obscured the mathematical principles upon which the analysis is based [8]. The regression line fitted to the data points is described by the equation $C_q = \log(N_q)/\log(E) - (1/\log(E)) \times \log(N_0)$ which is the log-transformed Eq. (1), rearranged to show the linear dependence of C_q on $\log(N_0)$.

Determining the efficiency value from a standard curve has been described as simplified because the PCR efficiency may vary with input concentration [15]. The requirement that the efficiency is constant for each included sample is rarely achieved and verified [41]. Studies on the reproducibility of the standard curve-derived PCR efficiency with replicate standard curves show a large variation in values derived from these data sets [8,11,24,34].

The C_q values used to construct the standard curve result from a dilution series. For a typical dilution series (10 times dilution per step; four steps) the expected C_q values, at a PCR efficiency of 2, range over approximately 14 cycles. As will be shown in Section 2.4, at high C_q values, all C_q are negatively biased when the observed fluorescence is cumulative. The resulting standard curve will be parallel and the slope of the curve will result in the same PCR efficiency as when the amplification was monitored with a non-cumulative reporter.

However, when the C_q values for the least diluted samples are too low, the negative bias in these samples is less (see Section 2.4). These slightly overestimated C_q values will lead to a standard curve with a steeper slope and the derived efficiency will be too low. Because only the lowest C_q value of a dilution series will be affected, and C_q values below 10 cycles are very rarely used in a standard curve, this bias will have had minimal effects. In practice, the standard curve-derived efficiency can, therefore, be considered to be independent of the fluorescent chemistry used to monitor the PCR reaction. Similarly, the use of a concentration series as calibration curve to look-up the concentration of an unknown sample from its C_q is not affected because both calibration curve and sample C_q are similarly biased.

2.3.2. PCR efficiency derived from amplification curves

Alternatively, the PCR efficiency can be derived from a subset of data points in the exponential phase of the amplification curve of each individual sample. Such an efficiency value was used in the first radioactively monitored quantitative PCR experiments [42]. For data obtained by fluorescent monitoring of PCR amplification [43], several authors advocated the determination of the PCR efficiency from the slopes of individual amplification curves on a semi-logarithmic scale [34,44,45] or by non-linear fit of Eq. (1) to data points in the exponential phase [15,41,46]. Similarly, mean efficiency values per amplicon can be estimated by calculating the common slope of the data points in the exponential phase for a group of samples [47]. Although good agreement between results obtained with a standard curve-derived efficiency value and the mean of the efficiencies derived from individual amplification curves has been reported [48] other studies show that PCR analysis with the comparative C_q method or with standard curve-derived efficiency values give precise (low within group variation) but significantly biased results [9,11,49]. In contrast, qPCR analysis based on the PCR efficiencies derived from individual amplification curves per sample resulted in unbiased target quantities but gave high variation within groups [9,49]. The average of these efficiency value for all samples per amplicon was shown to result in unbiased gene expression results with low variation [9,11,24,45,50]. The estimation of the PCR efficiency from the slope of the exponential phase of the amplification curve, plotted on a log (fluorescence) scale is directly derived from the logarithmic transformation of

the basic kinetic equation of PCR (Eq. (1)) [34]. The application of this method seems, therefore, to be limited to non-cumulative fluorescence data [24].

However, the simulation of the estimation of the PCR efficiency from cumulative fluorescence data shows that the estimated PCR efficiencies are only positively biased when they are derived from subsets with low cycle numbers (Fig. 2C). Even with a low PCR efficiency of 1.4, already after 14 cycles, the estimation error is below 1%. With maximum PCR efficiency, this number of cycles is sufficient to reduce the bias to 0.1%.

Comparison of the observed PCR efficiency values between different heart tissue samples shows that the PCR efficiency distributions overlap per amplicon and sample (Fig. 3F). The PCR efficiencies estimated from the individual samples can, therefore, be considered to be independent of the tissue sample; observed PCR efficiencies seem to be drawn from a random distribution around the actual PCR efficiency of the amplicon [9,24]. Moreover, comparison of Figs. 2C and 3F shows that the predicted bias at low cycles is small compared to this experimental variation.

Estimation of the PCR efficiency from individual sample curves requires the observable exponential phase to be as long as possible (see Section 2.2). When the subset of data used for estimation of the PCR efficiency is scrutinized, the TaqMan® data show more variable slopes than the SYBR green data (compare Fig. 3C and D). This variability is reflected in the increased variance of the resulting PCR efficiencies (Fig. 3F). Note that plotting the data on a logarithmic scale is required to judge this efficiency variance from the individual amplification curves. Identical 'slopes' on a normal fluorescence axis [3] merely indicate that the transition into the plateau phase occurs in parallel.

These results show that when the PRC efficiency is derived from the slope of the amplification curves per sample the resulting PCR efficiency will be correct when the data points used are beyond cycle 15. With low PCR efficiency and high abundance samples, one should be aware that in early cycles, the cumulative fluorescence curve has a steeper slope than the non-cumulative curve, and this will lead to an overestimation of the derived PCR efficiency.

2.4. C_q determination

The second parameter that has to be derived from the qPCR data set is the quantification cycle (C_q) which is the fractional number of cycles needed to reach the quantification threshold (N_q). C_q values have been the mainstay of qPCR data analysis since the introduction of fluorescence monitoring of the PCR reaction [6,43]. The C_q value marks the position of the amplification curve on the cycle axis and is proportional to the logarithm of the initial target concentration at constant amplification efficiency. C_q values are also referred to as C_t or C_p but this is discouraged in the MIQE guidelines [4].

Recommendations for placing the quantification threshold vary in literature. Some authors place the threshold at the level where amplicon DNA just becomes detectable [8,35] or at least at the low end of the exponential phase [6,10,20]. Other papers describe the threshold setting as arbitrary [44,49] or recommend specific positions like the midpoint of the exponential phase [45]. High threshold settings have mostly been avoided because of the variation in plateau phase levels. However, it was also recommended to avoid the lower end, and even the middle, of the exponential phase, because this region is still influenced by baseline noise [41]. Because the threshold is used in calculation based on the exponential amplification of DNA, the threshold should intersect with the exponential phase of the amplification curve [19]. Note that the threshold level is sometimes called 'noise band' [6], 'benchmark' [50] or 'detection threshold' [51] thereby adding to the confusion on the issues of baseline, background, threshold and variation in qPCR data analysis.

Alternatively, a C_q value has been derived from individual amplification curves by determining the fractional cycle at which a second derivative of a smoothed curve fitted to a subset of the observed data points reaches its maximum [38,52]. This second derivative maximum (SDM) marks the cycle at which exponential amplification no longer can be sustained and the curve begins to taper into the plateau phase [53]. This method gained popularity because it does not involve any decision by the user [52]. However, although the fluorescence level at the second derivative maximum typically will be similar for a given set of reaction conditions, this method is based on the assumption that information in the curve shape is more predictive of the target quantity than the fluorescence levels at each cycle. A comparison of different C_q determination methods showed that in assays with variable baseline and plateau conditions the threshold method showed superior precision [53].

The validity of the use of the C_q value is tightly linked to the exponential nature of the PCR amplification. Obviously the quantification threshold will be reached in an earlier cycle when the monitored fluorescence accumulates. This effect can clearly be seen when the C_q values that are observed with a cumulative fluorescent probe are plotted against the C_q values resulting from non-cumulative monitoring of the same simulated samples (Fig. 2D). At high C_q the negative bias in the C_q becomes constant and is then given by Eq. (4). This C_{shift} is especially large when the PCR efficiency is low. At low efficiencies it also takes a large number of cycles to reach this constant C_{shift}. This is why the standard curve-derived efficiency will be biased when at low PCR efficiencies such low C_q values are included (see Section 2.3.1).

The relation between PCR efficiency and C_q value that is present in Fig. 2C is not observed in the analysis results of the quantitative PCR data (Fig. 3E). The non-cumulative SYBR green data, as well as the cumulative TaqMan® data show no correlation between PCR efficiency and C_q values.

Because of the cumulative nature of the fluorescence resulting from hydrolysis probes, the C_q values observed with these probes are lower than expected from their PCR kinetics. This shift is minimally 1 cycle when the PCR efficiency is 2, but lower PCR efficiency leads to a larger C_{shift} (Fig. 2D). The magnitude of this bias is similar to the error observed in C_q values between replicate measurements of the same sample, which is generally described to be low, especially when compared to operator, kit and probe differences [54]. Replicate measurements on the same sample show C_q differences of 0.2 [49] or 0.4 cycles [55]. Intra-assay coefficients of variation for replicate C_q values were reported in the order of 1% [20], 7 % [56] and 10% [36]. The last percentage translates into a standard deviation of 2 cycles. This comparison of the C_{shift} bias with random experimental error is partly flawed because random error is averaged out whereas a systematic bias does not, and may go unnoticed when no reference is available.

2.5. Correction of C_{shift}

Because ΔN and C_{shift} are fully dependent on the slope of the amplification curve in the exponential phase, a correction for this bias can be based on the constant PCR efficiency during this phase (Fig. 4). This PCR efficiency can be derived from a standard curve or from a subset of data points in the exponential phase of the amplification curves [34]. On a logarithmic fluorescence scale, the slope of the amplification curve is the logarithm of the PCR efficiency. Therefore, the known PCR efficiency can be used to calculate ΔN and C_{shift}. The sum of the observed C_q and C_{shift} results in a corrected C_q value, representing the value that would have been found when the same fluorescent dye had behaved non-cumulatively.

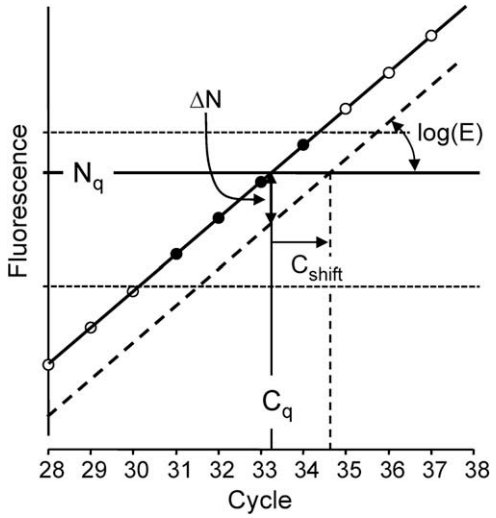

Fig. 4. Correction of C_q values determined from cumulative fluorescence curves. The circles represent the data points originating from monitoring the PCR reaction with a cumulative fluorescent probe. After setting the quantification threshold N_q (horizontal solid line) the C_q value can be determined. Using the estimated PCR efficiency value (E), the vertical distance to the equivalent non-cumulative fluorescence curve (dashed curve) can be calculated (Eq. (3)). Because the slope of both curves is equal to log(E), simple geometry suffices to calculate the horizontal distance (C_{shift}) between the curves. The observed C_q value of the cumulative fluorescence curve can then be corrected to the C_q value (vertical dotted line) that would have been observed when the fluorochrome had not accumulated. The figure also illustrates the setting a window-of-linearity [34] (horizontal dotted lines) which is used to determine the PCR efficiency of the current sample by linear regression using the data points in the window (black circles). Parameters: N_0: 1, PCR efficiency: 1.8. C_{shift} is 1.38 in this example.

This corrected C_q value can then be used to calculate the correct N_0 value. Note that in qPCR analysis algorithms that assume that the PCR efficiencies of all amplicons are equal, or at least similar enough to allow the difference to be ignored, like the comparative C_q method, the C_{shift} correction will have no effect on the result of the analysis.

The correction principle is illustrated in Fig. 4 and has to be applied to individual PCR samples. In case the PCR efficiency is derived from the individual amplification curves, the mean of all individual PCR efficiencies per amplicon has to be used to calculate the required C_{shift}. The latest version of the qPCR analysis program LinRegPCR (http://LinRegPCR.HFRC.nl) [24] implements this correction.

2.6. Calculate target quantity (N_0) and gene expression ratio

Although papers describing qPCR results often only report C_q values it is clear that interpretation of these results cannot be done without knowledge of the PCR efficiency values [57]; C_q values should not be compared as such but converted into and reported as target quantities [58]. Because of the exponential nature of PCR, small differences in PCR efficiency between amplicons can lead to large differences in C_q value whereas similar C_q values for different amplicons can represent very different target quantities when the PCR efficiencies differ between amplicons [11,24]. As stated above, an observed C_q of 30 cycles can represent a 5-fold difference in target quantity when the PCR efficiency of two amplicons differs only as much as from 1.9 to 2. Thus, restricting qPCR analysis to assays with a PCR efficiency above 1.9 will not prevent the variance introduced by ignoring the actual PCR efficiency. To avoid the tedious interpretation of C_q values it is recommended to use the estimated PCR efficiency, quantification threshold and C_q value to calculate a target quantity with the inverse of Eq. (1). The resulting N_0 value is an estimate of the target quantity in arbitrary fluorescence units.

Target quantities were calculated for simulated data sets monitored with non-cumulative and cumulative fluorescent chemistries (Fig. 5A). This simulation shows that the expected bias is dependent on the PCR efficiency because the vertical distance ΔN of the parallel curves is associated with a horizontal shift, C_{shift}, at the level of the quantification threshold (Eq. (4), Fig. 4). When the C_{shift} is ignored in PCR data analysis, biases will arise in the estimated target quantities (Eq. (5), Fig. 5A) and gene expression ratios (Eq. (6), Fig. 5B). The magnitude of these biases depends on the PCR efficiencies of the target and the reference genes. This effect is direct through the use of the efficiency value in calculating N_0 with the inverse of Eq. (1) and indirectly through the contribution of the efficiency to the C_{shift}. Fig. 5A shows that the bias in estimated N_0 values approaches the value calculated with Eq. (5) at high C_q. With low PCR efficiency, low C_q values show the largest bias. This is because in these circumstances, the non-cumulative and cumulative curves are not yet completely parallel and biased efficiency values will be estimated (Fig. 2C). Moreover, a low PCR efficiency results in a smaller ΔN but larger C_{shift} (Fig. 2D). With high PCR efficiencies, the bias in N_0 is constant and minimal at the maximum efficiency of 2.

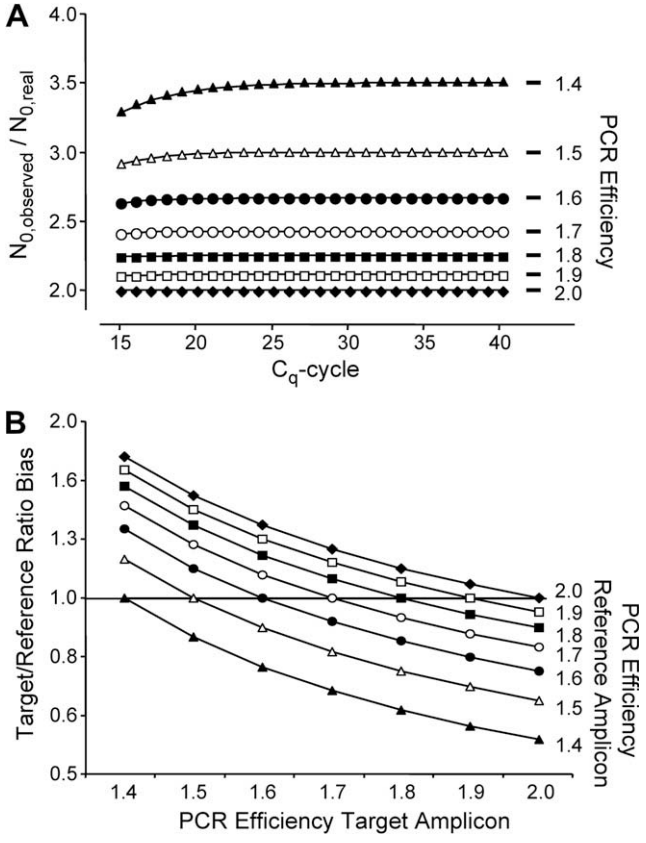

Fig. 5. Results are biased when the accumulation of fluorescence is ignored. (A) Although Eq. (5) (Section 4) predicts that the bias in the estimated target quantity (N_0) is independent of C_q, in practice N_0 is negatively biased when the C_q value, and thus the subset of data points used to calculate the PCR efficiency, is in the early cycles. To generate this graph, the C_q values and PCR efficiency values shown in Fig. 2C were used to calculate the observed N_0. The relative error in N_0 was then calculated as the ratio between observed and given N_0 value. This relative error is independent of N_0. Parameters: N_0: 0.000001, PCR Efficiency: 1.4–2.0. (B) The bias in the gene expression ratio, calculated by dividing the starting amount of a target gene by that of a reference gene in the same sample depends on difference between the PCR efficiencies of the target and reference amplicon (Eq. (6)). When the PCR efficiencies of both amplicons are equal, the gene expression ratio is unbiased. However, when the PCR efficiencies differ, positive and negative biases can occur. The parameters used in the calculation are the same as in Fig. 5A.

To study the effectiveness of the C_{shift} correction on the observed target quantity, its effect was simulated and the relative error in the resulting N_0 value was calculated (Fig. 6). This calculation shows that after the C_{shift} correction, for an amplicon with a PCR efficiency of 2, the N_0 values are within 0.5% of the given value already at a C_q of 12. With lower efficiency values, higher C_q values are required to reach the same small error. The dependence of the remaining error in N_0 on the C_q value results from the fact that at lower cycle numbers, the non-cumulative and cumulative amplification curves are not yet fully parallel (Fig. 2B). However, the observed remaining errors are well within the experimental and biological variation of quantitative PCR experiments [59,60].

Even when the accumulation of fluorescence is ignored, the gene expression ratio is unbiased when the PCR efficiencies of the target and the reference amplicon are equal (Fig. 5B). In that situation, the C_{shifts} cancel each other, resulting in unbiased gene expression ratios. For optimized PCR reactions, with efficiency values of 1.8 or higher, the bias in gene expression ratio will be limited to 12% (Fig. 5B). However, biases from 0.57 to 1.75 can be observed when these efficiencies range from 1.4 to 2. In this calculation of the bias in a gene expression ratio (Appendix C; Eq. (6)), a single reference gene is used. When the geometric mean of the expression levels of multiple reference genes is used for normalization of the target quantity [61], the resulting bias depends on the efficiency values of the individual reference genes. When these efficiencies are distributed around the PCR efficiency of the target amplicon, bias will be reduced.

Also the bias in the gene expression ratio can be removed by applying the described C_{shift} correction. Depending on the PCR efficiency and the C_q values, the C_{shift} correction procedure will completely remove the bias. When the PCR efficiencies of target and reference amplicons differ, some bias in the gene expression ratio may remain when C_q values are low.

The bias in the gene expression per sample as predicted by Eq. (6) is independent of the C_q values of the target and reference genes in the sample. This means that in a comparison of the relative difference of the gene expression ratios between different samples in an experiment the bias due to ignoring cumulative fluorescence cancels out; the same fold difference between samples would be obtained with or without C_{shift} correction. However, this result is only unbiased when the PCR efficiency values of target and reference amplicons were included in the calculations. Moreover, for the calculation of unbiased absolute differences between samples in an experiment the C_{shift} correction is required.

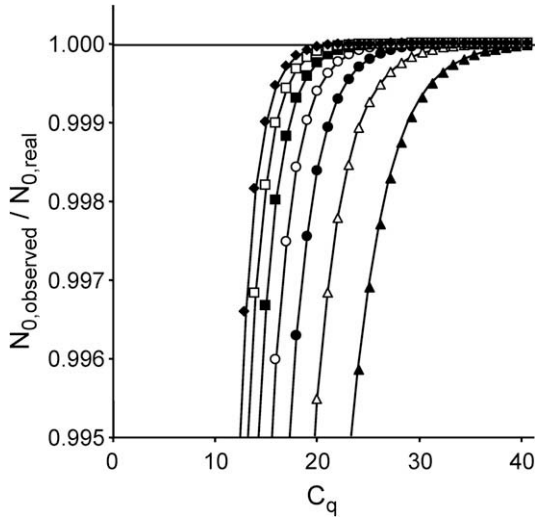

Fig. 6. C_{shift} correction does not remove all bias in N_0. The fact that the bias in N_0 is dependent on the C_q value (see Fig. 5A) makes that the C_{shift} correction illustrated in Fig. 4 is not removing the bias in all situations. After application of the correction to the data of Fig. 5A a small error in the estimated N_0 values remains present. The graph shows the remaining bias in these estimated N_0 values. The C_q values that have to be observed to restrict this bias to at most 0.5% are plotted for a range of PCR efficiency values. The graph shows that, to limit the error to 0.5% a C_q value above 22 is needed when the PCR efficiency was estimated to be as low as 1.4. However, most researchers aim to optimize their PCR reactions to PCR efficiencies of at least 1.8. Therefore, the C_{shift} correction allows C_q values as low as 14 before the estimation error rises above 0.5%.

2.7. Conclusions

Although monitoring PCR amplification with a cumulative fluorescent reporter gives higher observed fluorescence data, a correct PCR efficiency can be derived from the exponential phase from such a cumulative curve or from a standard curve based on C_q values derived from these data. The downward shift in C_q values is dependent on the PCR efficiency and can be corrected when this efficiency is known. When the accumulation of fluorescence is ignored, target quantities are at least 2-fold too high. However, the error in the target/reference ratio of starting quantities is small when the PCR efficiencies of the target and reference amplicons are similar. When PCR efficiencies are derived from the exponential phase of the amplification curves, the researcher should select a fluorophore–quencher pair with a high ΔR_n value to facilitate baseline estimation and thus reduce the variation in the estimated PCR efficiency.

3. Methods

3.1. Tissue samples

The tissue samples used in this study were taken from the hearts of three, one month old C57BL/6 mice. Atria were isolated, flash frozen in liquid nitrogen and stored at −80 °C for no more than 6 months prior to RNA isolation using a Trizol kit (Qiagen Inc., Invitrogen, Burlington, ON). RNA concentration was determined using a spectrophotometer (NanoDrop, Thermo Scientific), and quality was assessed by gel electrophoresis. A total of 500 ng of RNA was converted to cDNA using the high-capacity cDNA reverse transcription kit with random primers (Applied Biosystems Inc., Carlsbad, CA).

3.2. PCR reactions

C57BL/6 mouse atrial samples were amplified in 384-well plates on a BioRad cycler. The qPCR was performed using 15 µl reaction volumes. Specific primers for SYBR green qPCR were developed using Primer-BLAST (NCBI) and examined for secondary structures using the oligonucleotide calculator [62]. Custom oligo (Invitrogen) primers for β-actin reference (forward: CTGGAACG GTGAAGGCGACAG; Reverse: GCTTTTGGGAGGGTGAGGGAC; product: 182 bp), M2 muscarinic receptor (M2R) (forward: TAGCACCA TCAACCCTGCCTGC; reverse: TCCCCAAGACACACTCGACCAC; product: 151 bp), M3 muscarinic receptor (M3R) (forward: CACAAGC GAGTGCCTGAGC; reverse: GAATGGCCTCCCACCTGC; product: 115 bp) were used at a 1 µmol/l concentration in SYBR green Mastermix (Quanta). The amplification protocol was identical for all primer sets: 10 min 95 °C, 50× (15 s 95 °C, 30 s 60 °C, 30 s 72 °C). Hydrolysis probe-based studies used TaqMan® gene expression Assays-on-Demand from Applied Biosystems and AmpliTaq Gold® 360 PCR Master Mix (ABI). Sequence information for primer and probe assays are proprietary to ABI and thus not available for publication. β-actin, M2 muscarinic receptor and M3 muscarinic receptor used a FAM reporter (excitation = 495 nm, emission = 515 nm)

and TAMRA quencher (excitation = 565 nm, emission = 580 nm). These samples were measured in three parallel reactions using the following amplification protocol: 10 min 95 °C, 50× (15 s 95 °C, 30 s 60 °C, 30 s 72 °C).

3.3. Mathematical modeling

The basic equation for the kinetics of the exponential phase of PCR amplification (Eq. (1); Section 4) was used to derive an equation of the kinetics that would be observed when the fluorescence accumulates from cycle to cycle (Eq. (2)). These two models served to derive an equation for the distance between the cumulative and non-cumulative amplification curves on a log (fluorescence) scale. These equations were used in a spreadsheet program to calculate PCR efficiency values, target gene quantities and gene expression ratios. In these calculations, the PCR efficiency was derived from the slope of 4 data points (window-of-linearity method) [34]. A quantification threshold (N_q) was set at 1 cycle below the upper limit of this window. PCR efficiency and C_q values were then used to calculate the target quantity, N_0 [24]. The calculations were done with windows resulting in C_q values ranging from 10 to 40 cycles.

4. Theory/calculations

The basic equation for PCR kinetics is:

$$N_C = N_0 \times E^C \tag{1}$$

where the amount of amplicon after C cycles (N_c) is the starting concentration of the amplicon (N_0) times the PCR efficiency (E) to the power C. The PCR efficiency in this equation is defined as fold increase per cycle (2 indicates 100% efficiency). Because the fluorescence is linearly related to the amount of the amplicon, Eq. (1) also describes the increase in fluorescence for a non-cumulative DNA binding fluorochrome or hybridization reporter. When the fluorescent reporter of a hydrolysis probe is released during elongation, it remains fluorescent in subsequent cycles and accumulates. Because the amount of fluorescence released per cycle depends on the amount of amplicon present at the start of each cycle, cumulative fluorescence increases according to:

$$\Sigma N_C = \sum_{n=1}^{C} (N_0 \times E^n) \tag{2}$$

The practically constant vertical distance between Eqs. (1) and (2) at large cycle numbers, when plotted on a logarithmic axis (Fig. 2A), is written as ΔN, which can be calculated by:

$$\Delta N = \lim_{C\to\infty} (\Sigma N_C - N_C) = \log(1/(1-(1/E))) \tag{3}$$

Appendix A shows the derivation of Eq. (3). The horizontal distance, C_{shift}, between the cumulative and non-cumulative amplification curves then follows from the fact that on a logarithmic axis the slope of both lines can be considered to be given by $\log(E)$:

$$C_{\text{shift}} = \Delta N / \log(E) \tag{4}$$

When the accumulation of fluorescence is ignored, biases will occur in the estimation of the starting target quantity (N_0) or target/reference ratios in starting quantities. The bias in the target quantity, calculated as $N_0 = N_q/E^{C_q}$, is given by:

$$\frac{N_{0,\text{observed}}}{N_{0,\text{real}}} = E^{C_{\text{shift}}} = 1/(1-(1/E)) \tag{5}$$

and the bias in the gene expression ratio by:

$$\frac{R_{\text{observed}}}{R_{\text{real}}} = \frac{E_{\text{target}}^{C_{\text{shift,target}}}}{E_{\text{reference}}^{C_{\text{shift,reference}}}} \tag{6}$$

Derivation of the latter two equations is shown in Appendices B and C.

Acknowledgements

This work was supported in part by the Heart and Stroke Foundation of Ontario [DLJ]. JMT was the recipient of an Ontario Graduate Studies Studentship. The authors like to thank Maurice van den Hoff and Frank Beier for critically reading the manuscript and Alexandre Soufan for help with preparation of Fig. 3.

Appendix A. Derivation of ΔN (Eq. (3))

ΔN is defined as the distance between the logarithmic curves resulting from cumulative and non-cumulative fluorescence monitoring of PCR amplification. At high cycle numbers this distance approaches a limit of $\log(1/(1-(1/E)))$, because the distance at cycle number C is equal to the geometric series of $1/E$ up to $C-1$:

$$\begin{aligned}\log\left(N_0\sum_{n=1}^{C}E^n\right) - \log\left(N_0E^C\right) &= \log\left(N_0\sum_{n=1}^{C}E^n \Big/ N_0E^C\right)\\ &= \log\left(\sum_{n=1}^{C}E^n/E^C\right)\\ &= \log\sum_{n=0}^{C-1}(1/E)^n\end{aligned}$$

and

$$\lim_{C\to\infty}\log\sum_{n=0}^{C-1}(1/E)^n = \log(1/(1-(1/E)))$$

The latter equation requires that the PCR efficiency $E > 1$ which is always the case in quantitative PCR.

Appendix B. Derivation of the bias in N_0 when C_{shift} is ignored (Eq. (5))

The observed N_0 value, calculated with the C_q value of a cumulative fluorescence curve will be biased because the observed C_q value is too low due to the C_{shift} (Eq. (4)). The starting concentrations N_0 can be estimated from the quantification threshold (N_q), the PCR efficiency and the number of cycles (C_q) required to reach the threshold.

When the observed N_0 is give by: observed $N_0 = N_q/E^{C_q - C_{\text{shift}}}$ and the real N_0 is give by: real $N_0 = N_q/E^{C_q}$ and the bias in defined as the observed N_0 divided by the real N_0 then the bias is:

$$\begin{aligned}\text{bias} &= \text{observed } N_0/\text{real } N_0\\ &= N_q/E^{C_q-C_{\text{shift}}}/N_q/E^{C_q}\\ &= E^{C_q}/E^{C_q-C_{\text{shift}}}\\ &= E^{C_{\text{shift}}}\end{aligned}$$

With Eq. (4) for C_{shift} this bias simplifies to $1/(1-(1/E))$.

Appendix C. Derivation of the bias in the gene expression ratio when C_{shift} is ignored (Eq. (6))

The gene expression ratio is defined as the ratio of the estimated starting concentrations of a target and a reference gene:

$$\text{Ratio} = \frac{N_{0,\text{target}}}{N_{0,\text{reference}}} = \frac{N_q/E_{\text{target}}^{C_{q,\text{target}}}}{N_q/E_{\text{reference}}^{C_{q,\text{reference}}}} = \frac{E_{\text{reference}}^{C_{q,\text{reference}}}}{E_{\text{target}}^{C_{q,\text{target}}}}$$

The observed gene expression ratio, calculated with the C_q value of the cumulative fluorescence curves of target and reference genes

will be biased because the C_q values are too low due to the C_{shift} (Eq. (3)).

When the observed gene expression ratio is:

$$\text{Observed Ratio} = \frac{E_{\text{reference}}^{C_{q,\text{reference}} - C_{\text{shift,reference}}}}{E_{\text{target}}^{C_{q,\text{target}} - C_{\text{shift,target}}}}$$

and the real gene expression ratio is:

$$\text{real Ratio} = \frac{E_{\text{reference}}^{C_{q,\text{reference}}}}{E_{\text{target}}^{C_{q,\text{target}}}}$$

then the bias, defined as observed ratio divided by the real ratio is:

$$\begin{aligned}\frac{\text{observed Ratio}}{\text{real Ratio}} &= \frac{E_{\text{reference}}^{C_{q,\text{reference}} - C_{\text{shift,reference}}}}{E_{\text{target}}^{C_{q,\text{target}} - C_{\text{shift,target}}}} \Big/ \frac{E_{\text{reference}}^{C_{q,\text{reference}}}}{E_{\text{target}}^{C_{q,\text{target}}}} \\ &= \frac{E_{\text{reference}}^{C_{q,\text{reference}} - C_{\text{shift,reference}}}}{E_{\text{reference}}^{C_{q,\text{reference}}}} \Big/ \frac{E_{\text{target}}^{C_{q,\text{target}} - C_{\text{shift,target}}}}{E_{\text{target}}^{C_{q,\text{target}}}} \\ &= E_{\text{target}}^{C_{\text{shift,target}}} \Big/ E_{\text{reference}}^{C_{\text{shift,reference}}}\end{aligned}$$

References

[1] S.A. Bustin, V. Benes, T. Nolan, M.W. Pfaffl, J. Mol. Endocrinol. 34 (2005) 597–601.
[2] H.D. VanGuilder, K.E. Vrana, W.M. Freeman, BioTechniques 44 (2008) 619–626.
[3] T. Nolan, R.E. Hands, S.A. Bustin, Nat. Protoc. 1 (2006) 1559–1582.
[4] S.A. Bustin, V. Benes, J.A. Garson, J. Hellemans, J. Huggett, M. Kubista, R. Mueller, T. Nolan, M.W. Pfaffl, G.L. Shipley, J. Vandesompele, C.T. Wittwer, Clin. Chem. 55 (2009) 611–622.
[5] N.J. Walker, Science 296 (2002) 557–559.
[6] K.J. Livak, User Bulletin 2, PE Applied Biosystems, 1997.
[7] W.M. Freeman, S.J. Walker, K.E. Vrana, BioTechniques 26 (1999) 112–115.
[8] R.G. Rutledge, C. Cote, Nucleic Acids Res. 31 (2003) e93.
[9] Y. Karlen, A. McNair, S. Perseguers, C. Mazza, N. Mermod, BMC Bioinformatics 8 (2007) 131.
[10] M.W. Pfaffl, Nucleic Acids Res. 29 (2001) e45.
[11] J.H. Schefe, K.E. Lehmann, I.R. Buschmann, T. Unger, H. Funke-Kaiser, J. Mol. Med. 84 (2006) 901–910.
[12] S. Tyagi, D.P. Bratu, F.R. Kramer, Nat. Biotechnol. 16 (1998) 49–53.
[13] T. Wang, M.J. Brown, Anal. Biochem. 269 (1999) 198–201.
[14] J. Peccoud, C. Jacob, Biophys. J. 71 (1996) 101–108.
[15] A. Tichopad, M. Dilger, G. Schwarz, M.W. Pfaffl, Nucleic Acids Res. 31 (2003) e122.
[16] A. Batsch, A. Noetel, C. Fork, A. Urban, D. Lazic, T. Lucas, J. Pietsch, A. Lazar, E. Schomig, D. Grundemann, BMC Bioinformatics 9 (2008) 95.
[17] D.V. Rebrikov, D.I. Trofimov, Appl. Biochem. Microbiol. 42 (2006) 455–463.
[18] J. Wilhelm, A. Pingoud, M. Hahn, Anal. Biochem. 317 (2003) 218–225.
[19] J. Wilhelm, A. Pingoud, ChemBioChem 4 (2003) 1120–1128.
[20] A. Larionov, A. Krause, W. Miller, BMC Bioinformatics 6 (2005) 62.
[21] T. Bar, A. Stahlberg, A. Muszta, M. Kubista, Nucleic Acids Res. 31 (2003) e105.
[22] R.G. Rutledge, Nucleic Acids Res. 32 (2004) e178.
[23] R.G. Rutledge, D. Stewart, BMC Biotechnol. 8 (2008) 47.
[24] J.M. Ruijter, C. Ramakers, W.M. Hoogaars, Y. Karlen, O. Bakker, M.J. van den Hoff, A.F. Moorman, Nucleic Acids Res. 37 (2009) e45.
[25] B. Kaltenboeck, C. Wang, Adv. Clin. Chem. 40 (2005) 219–259.
[26] J.E. Noble, L. Wang, K.D. Cole, A.K. Gaigalas, Biophys. Chem. 113 (2005) 255–263.
[27] S.A. Marras, Mol. Biotechnol. 38 (2008) 247–255.
[28] R.P. Haugland, J. Yguerabide, L. Stryer, Proc. Natl. Acad. Sci. USA 63 (1969) 23–30.
[29] M.K. Johansson, Methods Mol. Biol. 335 (2006) 17–29.
[30] E. Reynisson, M.H. Josefsen, M. Krause, J. Hoorfar, J. Microbiol. Meth. 66 (2006) 206–216.
[31] S. Cikos, J. Koppel, Anal. Biochem. 384 (2009) 1–10.
[32] K.J. Livak, T.D. Schmittgen, Methods 25 (2001) 402–408.
[33] D. Klein, Trends Mol. Med. 8 (2002) 257–260.
[34] C. Ramakers, J.M. Ruijter, R.H. Lekanne Deprez, A.F.M. Moorman, Neurosci. Lett. 339 (2003) 62–66.
[35] M.L. Wong, J.F. Medrano, BioTechniques 39 (2005) 75–85.
[36] M.W. Pfaffl, G.W. Horgan, L. Dempfle, Nucleic Acids Res. 30 (2002) e36.
[37] J. Meijerink, C. Mandigers, L. van de Locht, E. Tonnissen, F. Goodsaid, J. Raemaekers, J. Mol. Diagn. 3 (2001) 55–61.
[38] R. Rasmussen, in: S. Meuer, C. Wittwer, K. Nakagawara (Eds.), Rapid Cycle Real-Time PCR: Methods and Applications, Springer, Heidelberg, 2001, pp. 21–34.
[39] O. Nordgard, J.T. Kvaloy, R.K. Farmen, R. Heikkila, Anal. Biochem. 356 (2006) 182–193.
[40] M. Simard, E. Boucher, P.R. Provost, Y. Tremblay, Anal. Biochem. 362 (2007) 142–144.
[41] S. Zhao, R.D. Fernald, J. Comput. Biol. 12 (2005) 1047–1064.
[42] R.J. Wiesner, Nucleic Acids Res. 20 (1992) 5863–5864.
[43] C.T. Wittwer, M.G. Herrmann, A.A. Moss, R.P. Rasmussen, BioTechniques 22 (1997) 130–138.
[44] A. Gentle, F. Anastasopoulos, N.A. McBrien, BioTechniques 31 (2001). 502, 504–506, 508.
[45] S.N. Peirson, J.N. Butler, R.G. Foster, Nucleic Acids Res. 31 (2003) e73.
[46] W. Liu, D.A. Saint, Anal. Biochem. 302 (2002) 52–59.
[47] P. Cook, C. Fu, M. Hickey, E.S. Han, K.S. Miller, BioTechniques 37 (2004) 990–995.
[48] E.J. Walsh, C. King, R. Grimes, A. Gonzalez, Biomed. Microdev. 8 (2006) 59–64.
[49] J.H. Marino, P. Cook, K.S. Miller, J. Immunol. Methods 283 (2003) 291–306.
[50] S. Cikos, A. Bukovska, J. Koppel, BMC Mol. Biol. 8 (2007) 113.
[51] E.J. Kontanis, F.A. Reed, J. Forensic Sci. 51 (2006) 795–804.
[52] V. Luu-The, N. Paquet, E. Calvo, J. Cumps, BioTechniques 38 (2005) 287–293.
[53] J.D. Durtschi, J. Stevenson, W. Hymas, K.V. Voelkerding, Anal. Biochem. 361 (2007) 55–64.
[54] S.A. Bustin, J. Mol. Endocrinol. 29 (2002) 23–39.
[55] P.Y. Muller, H. Janovjak, A.R. Miserez, Z. Dobbie, BioTechniques 32 (2002) 1372–1379.
[56] M.W. Pfaffl, M. Hageleit, Biotechnol. Lett. (2001).
[57] S.A. Bustin, Why the need for qPCR publication guidelines? – the case for MIQE, Methods, this Issue.
[58] S.A. Bustin, R. Mueller, Clin. Sci. 109 (2005) 365–379.
[59] A. Tichopad, R. Kitchen, I. Riedmaier, C. Becker, A. Stahlberg, M. Kubista, Clin. Chem. 55 (2009) 1816–1823.
[60] J.D. Combes, G. Grelier, M. Laversanne, N. Voirin, S. Chabaud, R. Ecochard, C. Lasset, C. Moyret-Lalle, Anal. Biochem. 393 (2009) 29–35.
[61] J. Vandesompele, P.K. De, F. Pattyn, B. Poppe, R.N. Van, P.A. De, F. Speleman, Genome Biol. 3 (2002) RESEARCH0034.
[62] W.A. Kibbe, Nucleic Acids Res. 35 (2007) W43–W46.